

A comparative *ab initio* study of the ferroelectric behaviour in KNO_3 and CaCO_3

M K Aydinol^{1,4}, J V Mantese² and S P Alpay³

¹ Metallurgical and Materials Engineering Department, Middle East Technical University, Ankara 06531, Turkey

² United Technologies Research Center, East Hartford, CT 06108, USA

³ Materials Science and Engineering Program and Institute of Materials Science, University of Connecticut, Storrs, CT 06269, USA

E-mail: kadri@metu.edu.tr

Received 24 July 2007, in final form 26 September 2007

Published 12 November 2007

Online at stacks.iop.org/JPhysCM/19/496210

Abstract

Potassium nitrate exhibits a reentrant phase transformation, where a metastable ferroelectric phase ($\gamma\text{-KNO}_3$) is formed upon cooling from high temperature. The layered structure of this ferroelectric phase is composed of alternating layers of potassium ions and nitrate groups; wherein, a central nitrogen atom is coordinated by three equilateral triangular oxygen atoms. The group layer is located less than midway between the cation layers, giving rise to a polar structure. From a structural perspective, the calcite phase of calcium carbonate looks quite similar to this ferroelectric phase; however, it does not exhibit a ferroelectric transition. In this work we have performed an *ab initio* computational analysis to study the: structural stability, electronic characteristics, and bonding of various phases and ferroelectric properties of CaCO_3 and KNO_3 . We find that both material systems have mixed covalent and ionic bonding. The covalent interactions are within the group atoms of carbonate and nitrate atoms while the ionic interactions occur between the negatively charged (carbonate or nitrate) group and the calcium or potassium cations. For the low temperature stable phase of CaCO_3 (calcite), however, there is a slight covalency between the cations and the oxygen atoms of the group. This latter interaction results in the crystallization of CaCO_3 in the calcite form and prevents a ferroelectric transition. We suggest that, in analogy to KNO_3 , a metastable form of CaCO_3 may also exist, similar to the phase of $\gamma\text{-KNO}_3$ that should have a spontaneous polarization equal to $30.6 \mu\text{C cm}^{-2}$, twice that of $\gamma\text{-KNO}_3$. Moreover, our analysis indicates that this material should have a coercive field smaller than that of $\gamma\text{-KNO}_3$.

(Some figures in this article are in colour only in the electronic version)

⁴ Author to whom any correspondence should be addressed.

1. Introduction

Ferroelectric potassium nitrate (KNO_3) possesses many of the characteristics of an ideal electrical switch: a true hysteresis field threshold, a squareness ratio often greater than 500, very low permittivity, high resistivity and low loss, and a modest spontaneous polarization [1, 2]. Indeed, KNO_3 was initially viewed as a candidate material from which to construct non-volatile random access memory (FRAM) devices; with early efforts aimed at commercializing this technology for defence applications. However, KNO_3 has three significant shortcomings that make it unsuitable for FRAM devices:

- (1) the ferroelectric state near room temperatures and ambient pressures is unstable, leading to a relaxation of the lattice to the non-ferroelectric aragonite phase;
- (2) it melts at relatively low temperatures (337 °C) and is water soluble, making its deposition and metallization difficult to integrate with IC processing;
- (3) it contains potassium, which has high mobility in Si, further complicating its integration with IC processing.

What has long been sought, therefore, is an analogous ferroelectric material that possesses many of the electrical attributes of ferroelectric KNO_3 , but is not constrained by its physical processing and compatibility limitations.

Ferroelectric KNO_3 is one of the polymorphic forms of KNO_3 and has been the subject of many experimental [3–8] and theoretical [9–11] studies. The existence of the polymorphic structures was first established by Bridgeman [12] and then by others [13, 14]. At ambient temperatures and pressures KNO_3 adopts the orthorhombic aragonite structure (α -phase or phase II). When heated, α -phase undergoes a transition at 128 °C to a trigonal structure (β -phase or phase I) that was earlier associated with the calcite structure [15], though it is now agreed that this conclusion is incorrect [16].

Upon cooling from the β -phase, KNO_3 does not transform directly back into the α -phase, but another trigonal structure (γ -phase or phase III) that comes into existence between 124 and 110 °C. Further cooling causes a reversion into the α -phase. This γ -phase is ferroelectric, with a spontaneous polarization along its c -axis [2]. Based on an early structural analysis [17] of the γ -phase, Sawada *et al* [18] estimated the spontaneous polarization to be $11 \mu\text{C cm}^{-2}$, which compares well with their own experimentally measured values of 8–10 $\mu\text{C cm}^{-2}$, as determined by hysteresis-loop and pyroelectric measurements. Ferroelectric behaviour was also observed [1] at room temperature in thick KNO_3 films, a consequence of the existence of the metastable γ -phase. The measured spontaneous polarization for these materials was $3.5 \mu\text{C cm}^{-2}$, though the ferroelectric state was also unstable and vanished within a few hours after formation. It is now accepted that, thick and thin film KNO_3 exhibits ferroelectric behaviour at much lower temperatures than bulk material, with transition time to the α -phase a function of film thickness [8]. Indeed, it has been shown that for suitably passivated, and very thin films of KNO_3 , the ferroelectric state may be maintained for several years; arguing for its use in non-volatile memory elements were the material not sensitive to water and the high mobility of the potassium ions would still not pose significant problems.

Molecular dynamics simulations of phase transitions, based on the potentials calculated from the Gordon–Kim modified electron gas formalism [10, 11], reveal that both the $\alpha \rightarrow \beta$ and $\gamma \rightarrow \beta$ phase transitions are initiated by the nearly free rotations of the nitrate ions about the c -axis which were seen as closely connected to the abnormal thermal expansion of the c -axis. In a separate study, a technique was developed for performing simulations at constant polarization in the context of first-principles calculations [9, 19]. This method was employed to map the energy landscape as a function of polarization in γ - KNO_3 [9], predicting a spontaneous

Table 1. Crystal structure data of aragonite CaCO₃, from [22].

Space group	<i>Pmcn</i> (62)					
Cell parameters	$a = 4.9598(5) \text{ \AA}$, $b = 7.9641(9)$, $c = 5.7379(6) \text{ \AA}$					
	Atom	Wyckoff	SOF	x	y	z
Atomic positions	Ca	4c	1	0.25000	0.58507(5)	0.25974(6)
	C	4c	1	0.25000	0.2386(2)	0.4148(3)
	O	4c	1	0.25000	0.0770(2)	0.4043(2)
	O	8d	1	0.4737(2)	0.3196(1)	0.4131(2)

Table 2. Crystal structure data of aragonite KNO₃, from [23].

Space group	<i>Pmcn</i> (62)					
Cell parameters	$a = 5.4142 \text{ \AA}$, $b = 9.1654$, $c = 6.4309 \text{ \AA}$					
	Atom	Wyckoff	SOF	x	y	z
Atomic positions	K	4c	1	0.25000	0.4166(1)	0.7568(2)
	N	4c	1	0.25000	0.7548(1)	-0.0848(1)
	O	4c	1	0.25000	0.8902(1)	-0.0893(2)
	O	8d	1	0.4492(1)	0.6866(1)	-0.0849(1)

polarization of $16 \mu\text{C cm}^{-2}$, in disagreement with experimental results. This latter discrepancy was, however, attributed to the smaller volume for the unit cell in the theoretical analysis. In order to understand the effects of variations in lattice parameters on polarization, they had also calculated the polarization for the γ -KNO₃ crystal using its experimental lattice parameters keeping the volume constant but only relaxing the atomic positions. In this case the calculated spontaneous polarization was found to be $7.5 \mu\text{C cm}^{-2}$ which is closer to the experimentally observed value. Thus, whatever the cell size, the atoms in the crystal structure relaxed to new positions but maintained the crystal symmetry. Consequently, although the absolute value of the polarization changed, the ferroelectric behaviour and switching mechanism are not expected to be different. Furthermore, in this study, a double-well potential was obtained for the dependence of energy of the ferroelectric phase on polarization. The change of polarization from negative to positive was found to be due to the movement of the NO₃ group of atoms parallel to the c -axis, and was accompanied by a 60° rotation of the group in their plane.

The ionic polarizabilities of NO₃⁻ in KNO₃ [20] and CO₃²⁻ in CaCO₃ [21], based on the point dipole model, were calculated to be very close to each other and it was conjectured that [21] CaCO₃ might also be ferroelectric. In addition, the similarity of the structures of KNO₃ and CaCO₃, gives rise to the intriguing questions: What would be the properties of a ferroelectric phase of CaCO₃, and how might we identify it experimentally? Such a material would be an ideal ferroelectric memory material since CaCO₃ is: not water soluble, has no mobile ion species and would undoubtedly have low dielectric constant compared to perovskite oxides.

The aragonite structure is common to both the KNO₃ and CaCO₃ compounds which have an orthorhombic space group *Pmcn*, with only slight differences in the representation of their atomic positions. In tables 1 and 2, the experimental data for CaCO₃ [22] and KNO₃ [23] in their aragonite forms, respectively, is given and the corresponding crystal structures can be seen in figures 1(a) and (b). The volume of the KNO₃ in the aragonite is approximately 30% larger than CaCO₃ aragonite. Another difference is that aragonite is the stable phase of KNO₃ at room temperature, whereas it is a high pressure polymorph of CaCO₃. The stable room temperature

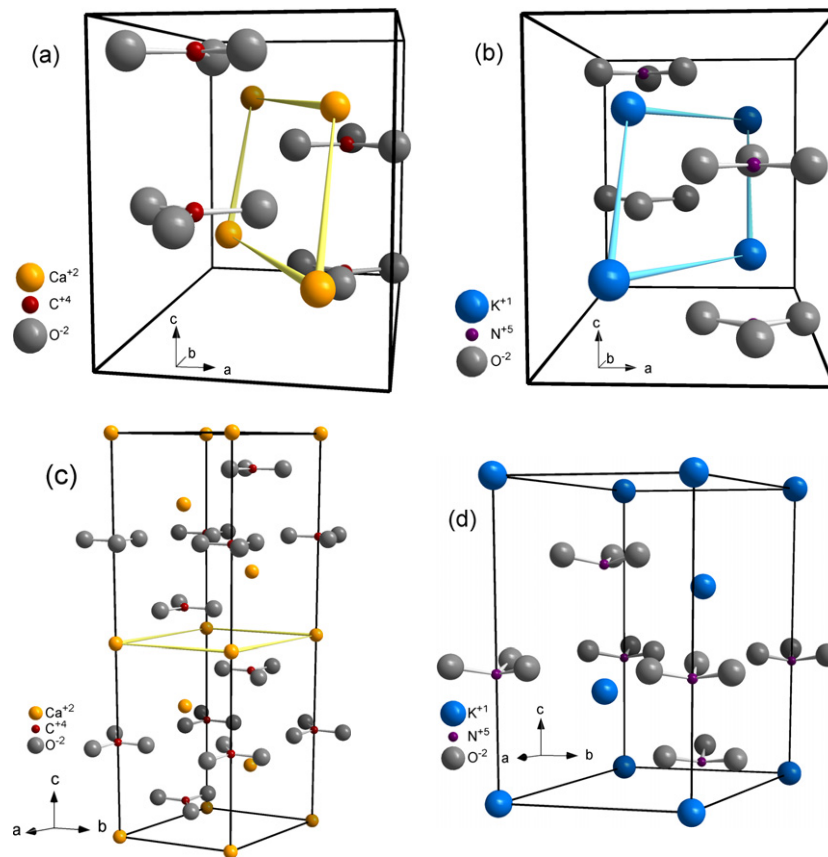


Figure 1. Experimental crystal structure views of CaCO_3 (a) aragonite, (c) calcite and KNO_3 (b) aragonite, (d) γ -phase.

Table 3. Crystal structure data of calcite CaCO_3 , from [24].

Space group	$R\bar{3}c$					
Cell parameters	$a = 4.988(2) \text{ \AA}, c = 17.068(2) \text{ \AA}$					
	Atom	Wyckoff	SOF	x	y	z
Atomic positions	Ca	6b	1	0	0	0
	C	6a	1	0	0	0.25
	O	18e	1	0.25700(6)	0	0.25

phase of CaCO_3 is calcite, while naturally occurring aragonite CaCO_3 can remain in this metastable form for millions of years, suggesting that other metastable phases may likewise be long lived. Calcite has a trigonal lattice in the $R\bar{3}c$ space group with the experimental lattice parameters [24] given in table 3, with a crystal structure shown in figure 1(c). There are several experimental and theoretical studies [25, 26] regarding the phase transitions in this system for the understanding of the geochemical cycle of carbon. In table 4, the experimental crystal structural data [16] is provided for the γ -phase of KNO_3 (space group $R3m$, see figure 1(d)).

First principles density functional theory (DFT) calculations have long been used in the field of condensed matter physics and materials science for the understanding of phase stability

Table 4. Crystal structure data of γ -phase KNO_3 , from [16].

Space group	$R3m$ (160)					
Cell parameters	$a = 5.487(1) \text{ \AA}$, $c = 9.156(3) \text{ \AA}$					
	Atom	Wyckoff	SOF	x	y	z
Atomic positions	K	3a	1	0	0	0.0000
	N	3a	1	0	0	0.405(6)
	O	9b	1	0.131(2)	-0.131(2)	0.434(3)

and transitions, electronic and crystal structure determination, phonon dispersion relations, elastic constant estimation and for predicting the properties of heretofore unknown materials. For ferroelectrics, expressions determining the dielectric and piezoelectric tensors have been a mainstay of such theoretical calculations. Born effective charges (BECs), polarization assessment and its derivatives have utilized density functional perturbation (DFPT) [27] calculations but subsequently transitioned to a modern theory of polarization using Berry phase formalism [28, 29]. The calculation of a macroscopic polarization as a Berry phase is a standard feature in many electronic structure codes like ABINIT [30]. ABINIT is a planewave pseudopotential DFT code, a common project of the Université Catholique de Louvain, Corning Incorporated, and other contributors. The applications of these techniques for the understanding of ferroelectric behaviour in materials were summarized in recent review articles [31, 32].

2. Methodology

In this study, we investigated the stability of various forms of CaCO_3 and in KNO_3 and determined the electronic structure of those phases using SIESTA [33, 34], a pseudopotential self-consistent DFT code with local orbital basis. Local density approximation (LDA), was assumed for the exchange correlation functional and Troullier–Martins [35] types of pseudopotentials were generated, where for the alkali elements semi-core states were also treated in the valence including partial core corrections. The double zeta basis set was used in the calculations along with the 300 Ryd mesh cut-off for the grid. In the calculations of KNO_3 , polarization orbitals were also included in the basis set. Brillouin zone sampling of the crystal structures were made by a Monkhorst–Pack mesh $16 \times 16 \times 16$, $10 \times 10 \times 10$, and $12 \times 8 \times 12$ k -points for the γ -phase, calcite and aragonite structures, respectively.

In addition, by using the Berry approach and the method of Souza *et al* [36] to calculate the exact ground state of an insulator in the presence of an electric field, as it was implemented in the ABINIT package by Veithen *et al* [37], we have calculated the optical dielectric constants and BEC tensors in these compounds. Finally, the dependence of crystal energy in the aragonite, calcite, and γ -phase compounds on the polarization was mapped by an approximate method developed by Sai *et al* [19] as was also implemented in the ABINIT package. For the calculations within the LDA, the Fritz–Haber-Institute pseudopotentials [38] were used as they are distributed in the ABINIT package and the wavefunctions were expanded in plane waves up to a kinetic energy cut-off of 35 Ha and the Brillouin zone was sampled using a $6 \times 6 \times 6$ Monkhorst–Pack mesh of special k -points for all systems investigated.

The structures given in tables 1–4 for CaCO_3 and KNO_3 were set up (primitive cell parameters in the rhombohedral setting were used for the hexagonal structures) and entered into the SIESTA code. They were allowed to fully relax according to the atomic positions and cell parameters with an accuracy of 0.01 eV \AA^{-1} for forces and 0.5 GPa for stresses.

Table 5. Relaxed lattice parameters of CaCO₃ in aragonite, calcite, and γ -phase structures.

Aragonite		<i>Pm\bar{c}n</i>				
Total energy per unit formula		−2067.234 eV				
Cell parameters		$a = 4.896 \text{ \AA}, b = 7.878 \text{ \AA}, c = 5.399 \text{ \AA}$				
	Atom	Wyckoff	SOF	x	y	z
Atomic positions	Ca	4c	1	0.25	0.5853	0.2624
	C	4c	1	0.25	0.2366	0.4134
	O	4c	1	0.25	0.0714	0.3983
	O	8d	1	0.4805	0.3213	0.4099
Calcite		<i>R$\bar{3}$c</i>				
Total energy per unit formula		−2067.351 eV				
Cell parameters		$a = 4.981 \text{ \AA}, c = 15.902 \text{ \AA}$				
	Atom	Wyckoff	SOF	x	y	z
Atomic positions	Ca	6b	1	0	0	0
	C	6a	1	0	0	0.25
	O	18e	1	0.2627	0	0.25
γ -phase		<i>R$\bar{3}$m</i>				
Total energy per unit formula		−2066.959 eV				
Cell parameters		$a = 4.927 \text{ \AA}, c = 7.426 \text{ \AA}$				
	Atom	Wyckoff	SOF	x	y	z
Atomic positions	Ca	3a	1	0	0	−0.0093
	C	3a	1	0	0	0.4354
	O	9b	1	0.153	−0.153	0.4286

3. Structural results

The resulting lattice parameters and total energies per unit formula are provided in tables 5 and 6 for CaCO₃ and KNO₃, respectively. As can be seen from the total energies given in table 5, our calculations predict the calcite structure as the ground state of CaCO₃. The aragonite structure is the next most stable phase, and finally the least stable phase is the γ -phase which actually does not naturally exist in nature. The ground state analysis for KNO₃, however, reveals that the γ -phase rather than aragonite is more stable by an amount of approximately 0.021 eV per unit formula, although aragonite is the stable room temperature phase of KNO₃. This may be because of the relatively loose packing of the ions along the c -direction in both crystal structures, such that during the static optimization of the cell and the atomic parameters, a short c -axis arises. Such static calculations are carried out at 0 K, where the kinetic energy effect due to finite temperatures is zero. Similar results have been obtained in the literature. For example, Dieguez and Vanderbilt [9] reported that there is approximately 14% shortening of the KNO₃ structure, while Lu and Hardy [11] calculated a c lattice parameter approximately about 11% smaller than the experimental values. Similarly, a decrease of approximately $\sim 10\%$ in the c -axis was also observed for the aragonite phase [11]. In CaCO₃, however, the shortening of the c -axis was found not to be as drastic because the ions are more packed along the c -direction compared to KNO₃. Therefore, relaxation of KNO₃ in the aragonite and γ -phase with its loose packing may result in the abnormal reduction in the c -axis lattice parameter that gave rise to a discrepancy in the ground state analysis. However, a single point calculation optimizing only the electronic degrees of freedom, in the experimental lattice parameters of KNO₃, yielded a

Table 6. Relaxed lattice parameters of KNO₃ in aragonite, calcite and γ -phase structures.

Aragonite		<i>Pmcn</i>				
Total energy per unit formula		−2019.050 eV				
Cell parameters		$a = 5.265 \text{ \AA}, b = 8.874 \text{ \AA}, c = 5.534 \text{ \AA}$				
	Atom	Wyckoff	SOF	<i>x</i>	<i>y</i>	<i>z</i>
Atomic positions	K	4c	1	0.25	0.4182	0.7584
	N	4c	1	0.25	0.7569	−0.1173
	O	4c	1	0.25	0.8988	−0.1236
	O	8d	1	0.4576	0.6858	−0.1172
Calcite		<i>R$\bar{3}$c</i>				
Total energy per unit formula		−2018.787 eV				
Cell parameters		$a = 5.373 \text{ \AA}, c = 17.578 \text{ \AA}$				
	Atom	Wyckoff	SOF	<i>x</i>	<i>y</i>	<i>z</i>
Atomic positions	K	6b	1	0	0	0
	N	6a	1	0	0	0.25
	O	18e	1	0.2339	0	0.25
γ -phase		<i>R3m</i>				
Total energy per unit formula		−2019.070 eV				
Cell parameters		$a = 5.266 \text{ \AA}, c = 7.833 \text{ \AA}$				
	Atom	Wyckoff	SOF	<i>x</i>	<i>y</i>	<i>z</i>
Atomic positions	K	3a	1	0	0	0.0074
	N	3a	1	0	0	0.4236
	O	9b	1	0.1380	−0.1380	0.4214

stable aragonite phase by an amount of 0.93 eV, compared to the γ -phase. Finally, the calcite structure was found to have the highest energy, as expected, since there is no such KNO₃ polymorph.

A large anisotropy in the thermal expansion of KNO₃ and CaCO₃ is observed experimentally and is also consistent with dynamic simulations. Liu *et al* [25], for example, performed molecular dynamics (MD) simulations of structural phase transitions in calcite–CaCO₃. They observed that, as temperature increases, the carbonate group starts to rotate around the triad axis associated with the abnormally large expansion in the *c* direction, consistent with the experimental finding of Dove and Powell [39]. This behaviour was attributed to the coupling of group rotation to the translation parallel to the triad axis in which all groups are correlated to each other. Similarly, Lu and Hardy [11] investigated phase transitions in KNO₃ using first-principles MD. They found that the *c* lattice parameter of aragonite KNO₃ at 0 K was shorter than the experimental value; but the disagreement was reduced by 3.6% as the temperature was raised to 300 K. The thermal anisotropy in aragonite KNO₃ was experimentally observed by Nimmo and Lucas [16, 23]. They found that as the temperature changed from 25 to 100 °C, the *c*-axis increased by 1.28%. Similar behaviour was found for γ -KNO₃ in the MD simulations of Lu and Hardy [11]. Heating γ -KNO₃ from 140 to 180 K using MD resulted in the *c*-axis being increased by 8.9% while *a*-axis decreased by 1.9%. They stated that these structural transitions are initiated with the rotations of the nitrate groups.

After the full relaxation of ionic positions and cell volume, without the symmetry constraints of the crystal structures of the phases, the C–O and N–O distances in CO₃ and NO₃ groups, respectively, have almost the same values regardless of the crystal structure. The

C–O distance was calculated to be 1.30(5) Å for the aragonite, calcite, and γ -phases of CaCO₃, whereas the N–O distance is 1.25(8) Å for all phases of KNO₃. These calculated distances agree quite well with the experimental values in their most stable structures; 1.282 and 1.273 Å, respectively, with a discrepancy of less than 2%. In order to determine whether the relaxed structures have the relative symmetries of the crystal structures studied in this paper, we have used the FINDSYM software of Stokes *et al* [40], which is a computer program that finds all of the symmetry operations existing and then identifies the space group of the input structure. The relaxed structures, cell vectors and coordinates of atoms, were input to FINDSYM and accuracy was set to 0.001. It was found that, after relaxation the symmetry and thus the space group for all structures were not destroyed within the specified accuracy value. Another structural criterion, is the arrangement of the atoms in these groups. In the experimental description of the calcite–CaCO₃ structure, C and O atoms constitute a plane normal to the *c*-axis, whereas in γ -phase KNO₃ the N atom is not in the plane formed by three oxygen atoms, but displaced out of it along the *c*-axis by 0.266 Å. In our calculations, however, an almost planar NO₃ group geometry was obtained, where the out of plane displacement is only about 0.02 Å. Similarly, in the case of γ -CaCO₃ a planar arrangement was obtained with a displacement \sim 0.05 Å. Considering the arrangements of these groups in the crystal structures of calcite and γ -phase, they lie in the *a*–*b* plane with Ca or K ions being exactly above and below the centre of the carbonate or nitrate groups, respectively. Relaxation of the calcite structure in both compounds yielded an exact halfway location for the negatively charged group between the positively charged ions. In the γ -phase structure of both compounds, however, the groups are not located at halfway, thus giving rise to a spontaneous polarization along the *c*-direction.

4. Electronic structure results

The electronic density of states (DOS) plots for the compounds studied are given in figure 2, where the Fermi energy was shifted to zero as reference. Both CaCO₃ and KNO₃, in all their structures, were found to be insulators. The band gap energies were calculated to be 2.88, 3.93, and 3.30 eV in CaCO₃ for the aragonite, calcite, and γ -phase structures, respectively. We note here that DFT calculations typically underestimate the band gap. The corresponding calculated band gaps for KNO₃ are 1.68, 2.03, and 2.10 eV. In all structures of KNO₃ compared to CaCO₃, the states lying below the Fermi energy are split with a narrower dispersion of the energy states. In terms of the effect of crystal structure, there seems to be a larger extent of molecular hybridization in the aragonite structure that causes wider energy dispersion for the states. In addition, by analysing the partial density of states (PDOS), according to angular momentum components as given in figures 3 and 4, one can deduce that both top of the valence and bottom of the conduction bands are mainly of p type, almost irrespective of the crystal structure. The lower energy states around -8 eV were found to have a mixed character of p and s, which are due to C/N and O atoms in the structure, characterizing the s–p overlap.

Furthermore, the PDOS plots according to the angular momentum on an elemental species basis are given in figures 5 and 6 for the calcite structures only, where for the other structures studied, almost an identical picture was obtained in terms of elemental contributions to all states within each compound. In KNO₃ the lowest lying energy state shown is due to p states of K mixed slightly with the p orbital of O. Correspondingly, in CaCO₃, there is such a mixture of p orbitals of Ca and O but this time also with s of O, and the mixture is moderate. This state, therefore, lies several eV below that of KNO₃ and is not shown in the PDOS plots. In both compounds, the valence band is predominantly composed of O 2p orbitals while the conduction band is composed of a mixture of C/N 2p and O 2p orbitals. By performing a local density of states (LDOS) calculation, in an energy window specific to highest occupied

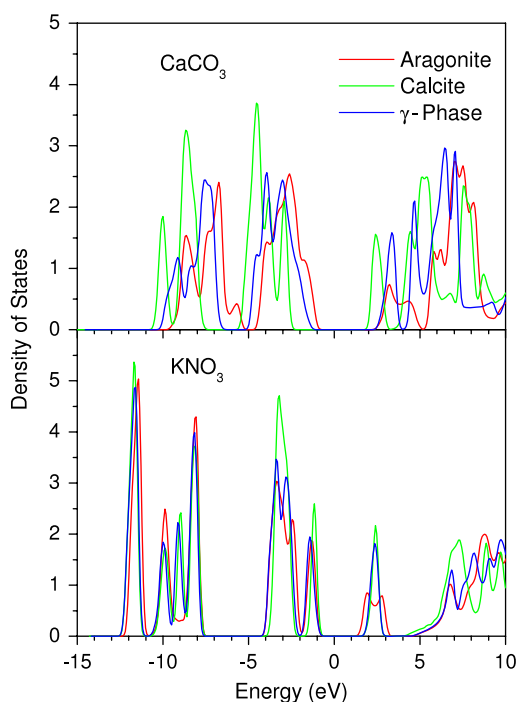


Figure 2. Total DOS of CaCO_3 and KNO_3 in all studied crystal structures.

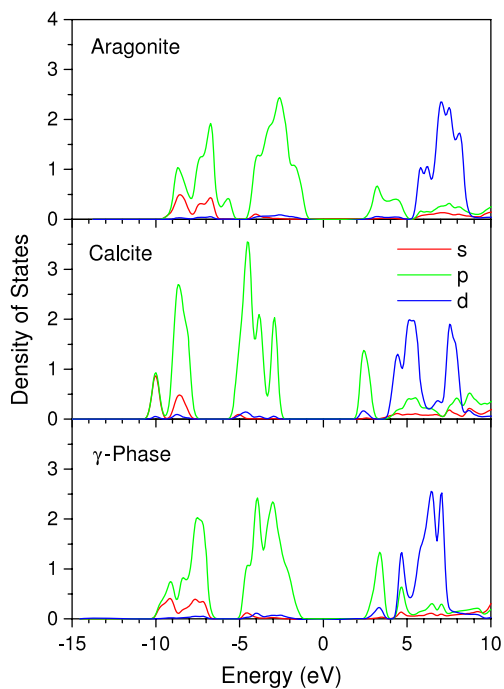


Figure 3. Angular momentum specific partial DOS of CaCO_3 in all studied crystal structures.

(HOMO) and lowest unoccupied (LUMO) molecular orbital states, the nature of the orbital picture is clarified in these compounds. In figure 7, LDOS figures for CaCO_3 (calcite) and KNO_3 (calcite and γ -phase), not only specific to HOMO and LUMO but also for other low

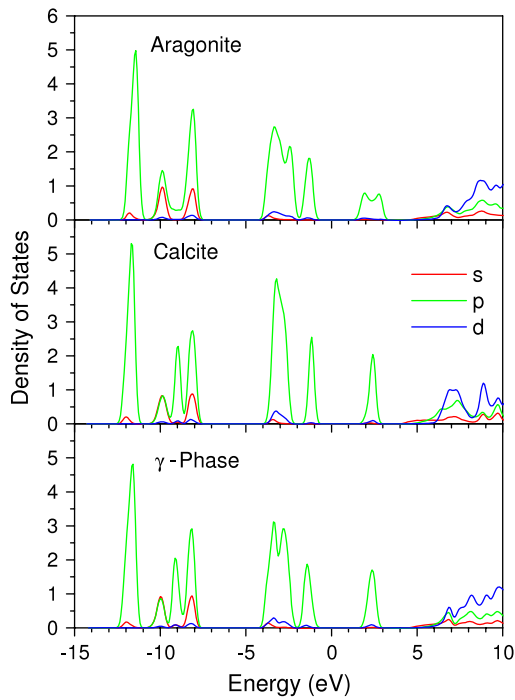


Figure 4. Angular momentum specific partial DOS of KNO_3 in all studied crystal structures.

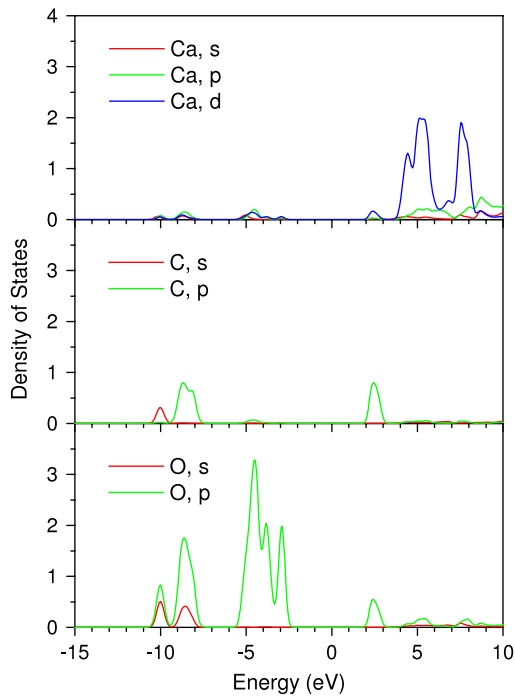


Figure 5. Angular momentum specific partial DOS of calcite- CaCO_3 on an elemental basis.

energy lying states, are given on the real space grid. The energy windows for these LDOS figures were set specifically for the peaks in the total DOS plot given in figure 8. In these figures, states located only around the carbonate or nitrate groups are shown, since they are the

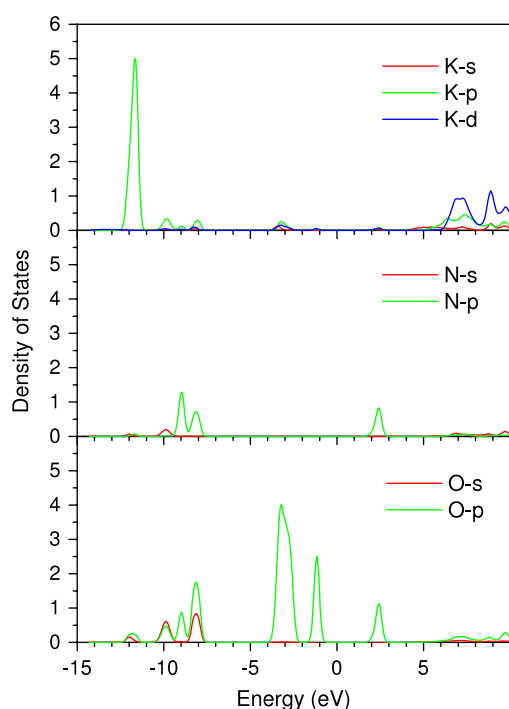


Figure 6. Angular momentum specific partial DOS of calcite-KNO₃ on an elemental basis.

only ones corresponding to the specified energy windows. It can clearly be seen now that for both compounds in all their possible crystal structures, p orbitals of O and C/N aligned along the *c*-axis of the crystal constitute the LUMO, in an anti-bonding π^* type of interaction, see figures 7(a₁), (b₁), and (c₁). In HOMO, however, there are only p orbitals of O, which are aligned in a triangular manner constituting the non-bonding orbitals, see figures 7(a₂), (b₂), and (c₂). In these orbitals, only excess p electrons of O reside and give rise to the mainly ionic interaction with the cation. Going down to lower energy states, there appear to be several differences between the bonding patterns of CaCO₃ and KNO₃. However, considering the effect of structure (calcite or γ -phase) on bonding in each compound, one can see that in KNO₃ there is almost no difference. Although the γ -phase was not shown explicitly in figure 7 for CaCO₃, the same principles apply for this compound with the exception that HOMO states are slightly different. The main difference between CaCO₃ and KNO₃ seems to be due to the low lying bonding and anti-bonding states. In CaCO₃, the bonding is σ type and it is between O p, s and C p orbitals, figure 7(a₄). In KNO₃, in addition to the above, there is one more type of bonding which is of π type and it is between O p and N p orbitals, figures 7(b₅) and (c₅). In terms of anti-bonding orbitals as shown in figures 7(a₆), (b₆), and (c₆) in CaCO₃ it is of σ^* type between O p and C s, and in KNO₃ it is again of σ^* type between O s and N s. Nevertheless, this will result in the covalent bond being somewhat stronger between N and O than the one between C and O. This actually shows itself in the bond lengths, N and O being slightly closer to each other compared to the C–O distance in any structure.

In figure 9, an electron density difference (self-consistently calculated electron density in the unit cell minus the superposition of the atomic charges) plot is provided for calcite CaCO₃. Almost an exact picture was obtained for other structures and for KNO₃ as well. The main

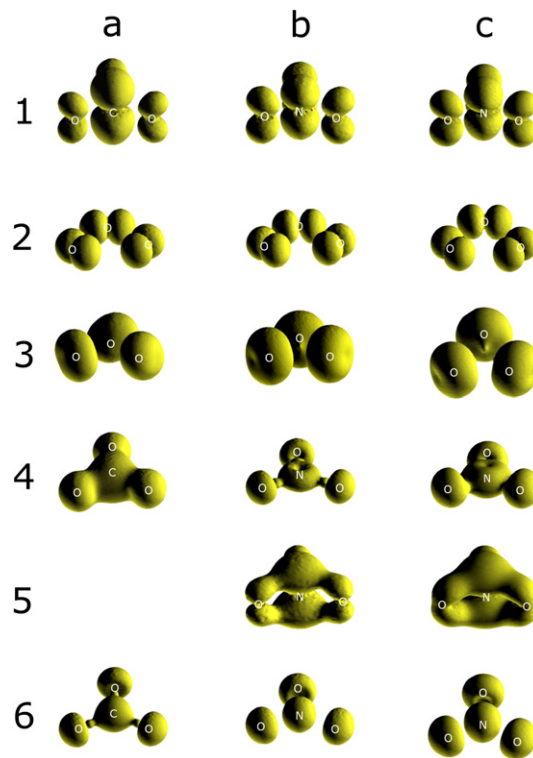


Figure 7. LDOS in the real space grid for (a) calcite- CaCO_3 , (b) calcite- KNO_3 and (c) γ -phase KNO_3 , where the energy windows were set to the specified states, shown as peaks in total DOS given in figure 8.

features that appear in this figure are the depletion of electrons from carbon in the angular regions between C–O directions and also from O in the region pointing towards C. There is also a charge accumulation around C in the region pointing towards O and also around O in regions aligned in a triangular manner, forming a two lobe shape which depicts the bonding pattern of the carbonate group as it is seen in figures 7(a₂), (b₂), and (c₂). A similar picture was also obtained in the literature for calcitic MgCO_3 [41] and CaCO_3 [42] compounds.

The analyses of the electronic structures in terms of the bonding and anti-bonding states show clearly the mixed ionic and covalent bonding in both CaCO_3 and KNO_3 . Within the carbonate or nitrate groups strong covalent bonds are formed which then ionically interact with the cations. A DFT study confirms [43] the ionic calcium–carbonate interaction and also shows that the charge on Ca is somewhat less than two.

The bonding picture given above, however, does not reveal much about the origin of ferroelectricity in γ -phase KNO_3 nor the reason why it is not observed in calcite- CaCO_3 . The studies, especially on ABO_3 perovskites, however, show that ferroelectric instability is very much related to the orbital hybridization between metal and oxygen orbitals. Thus there is some covalent character in bonding, yielding a second-order Jahn–Teller distortion. If the bonding in an ideal cubic perovskite were entirely ionic it would remain centrosymmetric, resulting in a non-ferroelectric behaviour. However, it is such that with Jahn–Teller distortion the symmetry of the structure is reduced and mixing of the bottom of the conduction band and the top of the valence band takes place which are initially of non-bonding character. This

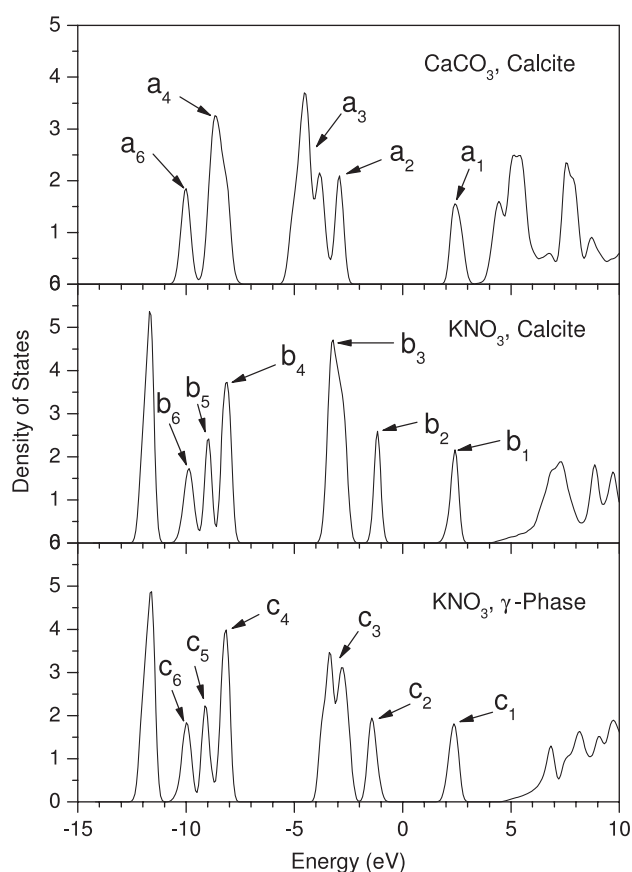


Figure 8. Total DOS of compounds specifying the states labelled as peaks that are used in LDOS analysis.

results in the valence and conduction band becoming more of bonding and anti-bonding type, respectively, giving rise to a widening of the band gap [44]. This ligand field stabilization mechanism was studied within DFT in perovskite BaTiO_3 [45] and in trigonal LiNbO_3 [46], where the ferroelectric distortion was ascribed to metal d -oxygen p covalent hybridization. However, the main bonding interactions in CaCO_3 and in KNO_3 are between C/N and O atoms. It appears that the states constituting HOMO and LUMO have a minor role or possibly no role in the ferroelectric behaviour observed in γ -phase KNO_3 , since there is almost no difference in these, within the structures studied, not only in KNO_3 but also in CaCO_3 .

The interaction between the carbonate/nitrate group and the cation, Ca or K , can be thought to be purely ionic and is expected to be due to oxygen p constituting the HOMO and the cation itself. Several studies [41, 42], however, have indicated the slight covalent nature of the bond between Ca/Mg and O in calcite/magnesite. This may have a significant role in the non-ferroelectric character of the calcite structures. We, therefore, performed Mulliken charge population analysis on the overlapping orbitals between nearest neighbour atoms. The results are given in table 7. It is again seen that irrespective of the crystal structures studied, the main charge overlap is between C/N and O atoms in $\text{CaCO}_3/\text{KNO}_3$ compounds. The charge overlap is of bonding nature and it is around 0.41 and 0.53 eu for CaCO_3 and KNO_3 , respectively, constituting the strong covalent bond between the species in the carbonate or nitrate group.

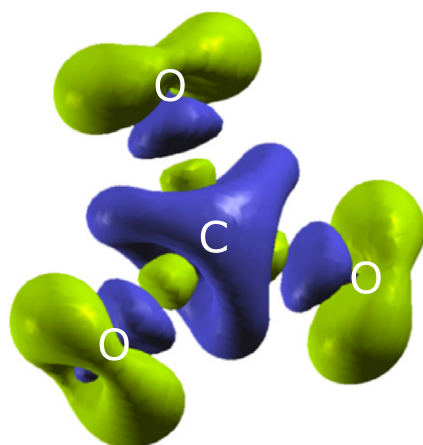


Figure 9. Difference in electron density between crystal and atomic superposition in the carbonate group of calcite CaCO_3 , showing the transfer of charge between carbon and oxygen atoms. Light (green) and dark (blue) colours indicate the accumulated and depleted regions of electronic charge, respectively.

Table 7. Mulliken population analysis in electron units in the regions of overlapping nearest neighbour atoms.

Phase	CaCO_3		KNO_3	
	Ca–O	C–O	K–O	N–O
Aragonite	0.127	0.422	0.102	0.534
Calcite	0.152	0.412	0.131	0.540
γ -phase	–0.017	0.414	–0.012	0.533

The overlap charge for a Ca/K and O pair, however, was found to be dependent on the crystal structure. For both the aragonite and calcite structures there is a considerable amount of charge accumulation (more than 0.1 eu) in the region between Ca/K and O. On the other hand, in the γ -phase there is a very slight anti-bonding character, which is due to charge depletion in the region between those species, indicating a stronger ionic type of interaction. This is apparently related to the differences in the arrangement of cations and carbonate and/or nitrate groups in the unit cells of these crystal structures. In a calcite structure, each cation is surrounded by six O atoms forming perfect corner sharing octahedrons, whereas in aragonite and γ -phase structures, the coordination is ninefold, see figure 10. The symmetry of the polyhedral shapes, however, is very different. In the aragonite structure it is quite complicated, whereas in the γ -phase structure each cation is sandwiched between planes formed by a network of O atoms. In the top plane of this polyhedral shape each cation resides with the O atoms arranged in an irregular hexagonal network, while in the bottom plane there is an equilateral triangular arrangement. It should be also noted that the vertical distance between the cation and the bottom triangular oxygen plane is approximately three times greater than the vertical distance from the top oxygen plane; although the interatomic distance between the cations and any bottom plane oxygen is shorter than the distance to any top oxygen plane. For example, in the relaxed γ -phase KNO_3 distances are 2.66 and 2.72 Å for potassium—bottom and top plane oxygen atoms, respectively. In calcite KNO_3 , however, the six-fold interionic distance is 2.57 Å. Because the Mulliken population strongly depends on the choice of the basis set, confirmation of covalency between the oxygen and the cation requires that the charge densities be calculated and contour

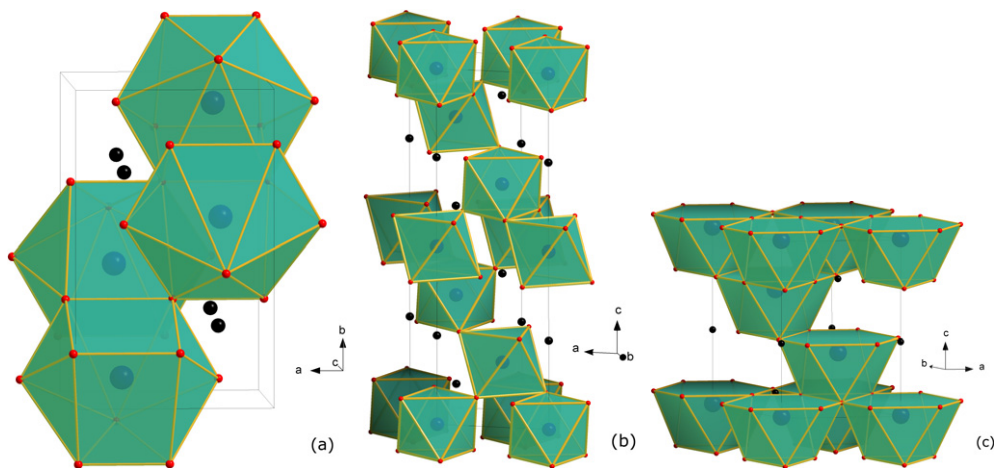


Figure 10. Oxygen coordination of cations in (a) aragonite, (b) calcite, and (c) in γ -phase structures.

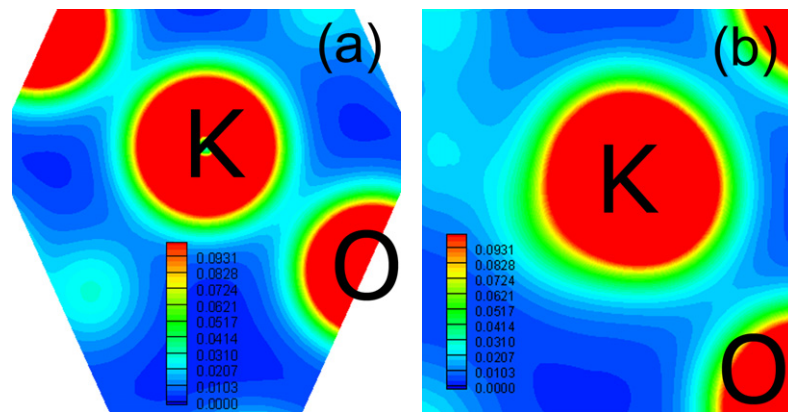


Figure 11. Charge density contour plots in crystal planes containing the shortest K and N atoms in (a) calcite and (b) γ -phase structures of KNO_3 .

plots constructed as shown in figure 11, though they are only shown for KNO_3 in calcite (figure 11(a)) and γ -phase (figure 11(b)) structures over crystal planes that contain potassium and oxygen atoms separated by the shortest distance. In the calcite structure, there is slightly more charge accumulation at the centre of the line connecting K (Ca) and O than the one in the γ -phase, which are 0.026 (0.045) eu bohr^{-3} and 0.017 (0.023) eu bohr^{-3} , respectively. The large discrepancy between the experimental and relaxed c lattice constants in structures may, however, make suspect the above conclusion. We therefore calculated the charge densities in calcite- CaCO_3 and γ - KNO_3 at their exact experimental structures, to determine whether the nature of the Ca/K–O bond changes compared to the relaxed condition. We found that the maximum value of the electronic charge at the centre of the bond between the constituent atoms did not change. However, the spatial distribution was found to be a little narrower. The difference in the Ca–O bond length between the experimental and relaxed structures came out to be only 3.1% in calcite- CaCO_3 , the experimental value being larger. In γ - KNO_3 the difference is more pronounced at 7.2%. Therefore, atoms being at the experimental positions,

Table 8. Stacking sequence of species along the c -axis of the crystal structures studied. \oplus and Δ represent the cation and the carbonate or the nitrate group, respectively. A, B, and C represent the usual positions for stackings in the triangular layers of atoms, whereas P and Q represent the corner and face centre positions of a rectangle, respectively. $-$ and \wedge represent the accompanied rotations of the groups around their normal axis as they are stacked, which are 0° and 60° , respectively.

Phase	Cation-Group	Cations only		Groups only	
Aragonite	$\oplus-\Delta-\Delta$	ABAB	\sim Triangular \sim Non-planar	$P^-Q^{\wedge}P^-Q$	Rectangular Planar
Calcite	$\oplus-\Delta$	ABCABC	Triangular Planar	$A^{\wedge}B^{\wedge}C^{\wedge}A^{\wedge}B^{\wedge}C$	Triangular Planar
γ -phase	$\oplus-\Delta$	ABCABC	Triangular Planar	$A^-B^-C^-A^-B^-C$	Triangular Planar

the reduction in the covalency of the bond between Ca and O should be very small in calcite– CaCO_3 . The K–O bond in γ - KNO_3 , however, should become more ionic with the difference between the character of the bonds in calcite– CaCO_3 and γ - KNO_3 , remaining independent as to whether they are at their DFT relaxed positions or experimentally observed positions. Although these charge densities are low and the chemical bond should be considered as primarily ionic, one can say that compared to the γ -phase, the calcite structure has a bond between the cation and the group that is less ionic because more charge is built up at the centre of the bond. This result may actually be because of the closer distance between the cation and the O atom in calcite structures.

The spontaneous polarization in the ferroelectric γ -phase KNO_3 was found [9] to be due to the movement of the NO_3 group parallel to the c -axis, which is related to a 60° rotation of the group. The possibility of this rotation depends very much on the crystal structure in terms of the stacking of the cations and the groups along the direction of the rotation. In table 8, the stacking sequence of cations and groups along the direction (c -axis of the crystal structures) that is parallel to the normal axis of the group are summarized. In terms of the stacking of the cation and the group, the calcite and γ -phase are the same, achieved by one alternating sequence; while in the aragonite structure two group layers (displaced relative to each other in the b -direction) are sandwiched between two cation layers. In the stacking sequence of cations, they form a perfect planar triangular network in the calcite and γ -phases, whereas in aragonite it is very slightly non-planar and irregular by an amount of approximately 1° . In terms of group stacking, the aragonite structure differs significantly from the other structures, such that it forms a rectangular network. The calcite and γ -phase groups, however, form a triangular network with ABC type of stacking similar to face centred cubic structures. The only difference between the calcite and γ -phase structure is the rotation of the groups as they are stacked in between the cation layers. In the calcite structure, groups are rotated by 60° around their normal axis, whereas in the γ -phase there is no such rotation. In figure 12, the orientations of the groups in between two hexagonal cation layers are given for the (a) calcite and (b) γ -phase structures. It can be seen that the orientation of the groups between the cation layers differs as well. In the γ -phase structure, groups are aligned in such a way that the projection of the oxygen branches of the group onto the underlying cation layer points to the centre of the cation–cation bond. With respect to this orientation, the group in the calcite structure is rotated by 30° clockwise making the O–cation bond distance shorter, which may be a consequence of slight covalency of the bond in the calcite structure. It should also be noted that the group in the calcite structure is halfway between the cation layers, while in the γ -phase the group is closer to the cation layer underneath.

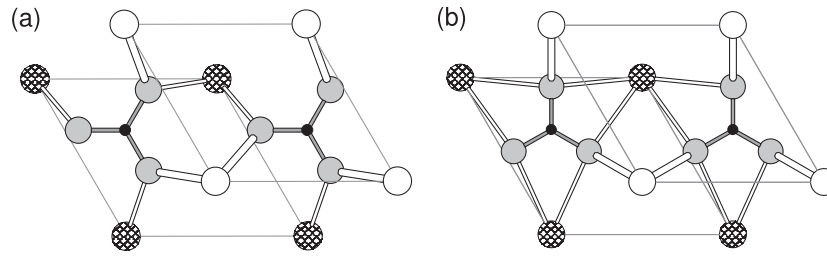


Figure 12. Top views of (a) calcite and (b) γ -phase structures showing the orientation of groups within hexagonal cation layers. The cross-hatched and open circles represent the cations that are located below and above the layer of the group, respectively.

Table 9. High frequency dielectric constants for CaCO_3 and KNO_3 in aragonite, calcite and γ -phase structures. Experimental values from [51] were given in parentheses.

Phase	CaCO_3 ($\epsilon_{xx}^\infty, \epsilon_{yy}^\infty, \epsilon_{zz}^\infty$)	KNO_3 ($\epsilon_{xx}^\infty, \epsilon_{yy}^\infty, \epsilon_{zz}^\infty$)
Aragonite	2.958, 2.992, 2.396 (2.841, 2.826, 2.340)	2.224, 2.247, 1.754 (2.277, 2.265, 1.774)
Calcite	2.708, 2.708, 2.132 (2.749, 2.749, 2.208)	2.252, 2.252, 1.695
γ -phase	2.950, 2.950, 2.295	2.459, 2.459, 1.803

5. Polarization calculations

For a material to be considered a ferroelectric it has to be a piezoelectric with two or more stable polarization states in the absence of an electric field; further, these states should be switchable by an applied electric field (spontaneous polarization). Several physical properties of the high symmetry phase: polarizability, dielectric constant, band gap, BECs [47], the splitting between the frequencies of the longitudinal optical and transverse optical phonons (LO–TO splitting) [48], etc, were correlated to ferroelectric phenomena and employed to predict whether a particular structure will distort spontaneously from this high symmetry paraelectric phase to yield ferroelectric behaviour. In this regard, we calculated, in the ABINIT relaxed structures, the high frequency (electronic) dielectric constants ϵ^∞ and BECs, Z^* , which are given in tables 9–12. While the calculated ϵ^∞ values are much lower than that of rocksalt chalcogenides [49], semiconductors, or perovskite oxides [50], there is a good agreement between the experimental values determined using the available index of refraction [51] of KNO_3 and CaCO_3 and the calculations (table 9). We also note that the dielectric constant for both compounds in all probable crystal structures is negatively uniaxial such that $\epsilon_{zz}^\infty/\epsilon_{xx}^\infty < 1$ as is the case for the ferroelectric phases of BaTiO_3 [50] and KNbO_3 [52].

The Born effective charge (BEC) concept is often interpreted as an indicator of ferroelectric instability; a large BEC gives rise to strong long-range ionic interactions that favour the ferroelectric instability [45]. The definition of BEC is the mixed second derivative of total energy with respect to electric field and atomic displacement. However, it is commonly regarded either as the derivative of the polarization with respect to atomic displacement at zero macroscopic field, or as the derivative of the force on an atom with respect to the macroscopic field at zero atomic displacement. Therefore, it is a dynamic quantity that can strongly be influenced by dynamic charges of orbital hybridization induced by atomic displacements. Consequently, it can take on anomalously large values [53], compared to static ionic charges

Table 10. Calculated Born effective charge (BEC) of the atoms in CaCO₃ and KNO₃ in the aragonite structure. The BEC of the same elements in the unit cell have identical amplitude except some sign change indicated by a \pm sign. Three oxygen BEC correspond to the oxygen ions in the carbonate or nitrate group.

Atom	CaCO ₃	KNO ₃
Ca/K	$\begin{pmatrix} 2.462 \\ 2.376 \pm 0.020 \\ \pm 0.171 \quad 2.202 \end{pmatrix}$	$\begin{pmatrix} 1.143 \\ 1.129 \pm 0.003 \\ \pm 0.077 \quad 1.013 \end{pmatrix}$
C/N	$\begin{pmatrix} 2.613 \\ 2.733 \pm 0.058 \\ \pm 0.063 \quad 0.570 \end{pmatrix}$	$\begin{pmatrix} 2.174 \\ 2.251 \pm 0.051 \\ \pm 0.042 \quad 0.322 \end{pmatrix}$
O	$\begin{pmatrix} -1.9756 & -0.4837 & \pm 0.0892 \\ -0.4837 & -1.4483 & \pm 0.0677 \\ \pm 0.1016 & \pm 0.0549 & -0.9305 \end{pmatrix}$	$\begin{pmatrix} -1.3648 & -0.4623 & \pm 0.0287 \\ -0.4460 & -0.8654 & \pm 0.0258 \\ \pm 0.0327 & \pm 0.0167 & -0.4472 \end{pmatrix}$
	$\begin{pmatrix} -1.1237 \\ -2.2124 \pm 0.0770 \\ \pm 0.0841 \quad -0.9108 \end{pmatrix}$	$\begin{pmatrix} -0.5883 \\ -1.6497 \pm 0.0062 \\ \pm 0.0138 \quad -0.4405 \end{pmatrix}$
	$\begin{pmatrix} -1.9756 & 0.4837 & \pm 0.0892 \\ 0.4837 & -1.4483 & \pm 0.0677 \\ \pm 0.1016 & \pm 0.0549 & -0.9305 \end{pmatrix}$	$\begin{pmatrix} -1.3648 & 0.4623 & \pm 0.0287 \\ 0.4460 & -0.8654 & \pm 0.0258 \\ \pm 0.0327 & \pm 0.0167 & -0.4472 \end{pmatrix}$

Table 11. Calculated BEC of the atoms in CaCO₃ and KNO₃ in the calcite structure. The BEC of the same elements in the unit cell have identical amplitude except some sign change indicated by a \pm sign. Three oxygen BEC correspond to the oxygen ions in the carbonate or nitrate group.

Atom	CaCO ₃	KNO ₃
Ca/K	$\begin{pmatrix} 2.399 \pm 0.2031 \\ \pm 0.203 \quad 2.399 \\ \quad \quad \quad 2.189 \end{pmatrix}$	$\begin{pmatrix} 1.118 \pm 0.114 \\ \pm 0.114 \quad 1.118 \\ \quad \quad \quad 1.002 \end{pmatrix}$
C/N	$\begin{pmatrix} 3.104 \\ 3.104 \\ \quad \quad \quad 0.334 \end{pmatrix}$	$\begin{pmatrix} 2.775 \\ 2.775 \\ \quad \quad \quad 0.183 \end{pmatrix}$
O	$\begin{pmatrix} -2.1663 & -0.5751 & -0.0672 \\ -0.5751 & -1.5022 & 0.1163 \\ -0.0675 & 0.1169 & -0.8411 \end{pmatrix}$	$\begin{pmatrix} -1.5943 & -0.5140 & -0.0105 \\ -0.5140 & -1.0008 & 0.0182 \\ -0.0099 & 0.0171 & -0.3953 \end{pmatrix}$
	$\begin{pmatrix} -1.1701 & \quad \quad \quad 0.1343 \\ \quad \quad \quad -2.4984 \\ 0.1350 & \quad \quad \quad -0.8411 \end{pmatrix}$	$\begin{pmatrix} -0.7040 & \quad \quad \quad 0.0210 \\ \quad \quad \quad -1.8911 \\ 0.0198 & \quad \quad \quad -0.3953 \end{pmatrix}$
	$\begin{pmatrix} -2.1663 & 0.5751 & -0.0672 \\ 0.5751 & -1.5022 & -0.1163 \\ -0.0675 & -0.1169 & -0.8411 \end{pmatrix}$	$\begin{pmatrix} -1.5943 & 0.5140 & -0.0105 \\ 0.5140 & -1.0008 & -0.0182 \\ -0.0099 & -0.0171 & -0.3953 \end{pmatrix}$

where this has been irrefutably attributed to partial covalence in the given material [54]. In this regard, an anomalously large BEC can arise either because of a tendency to ferroelectric distortion that necessitates a large stabilization in energy due to small atomic displacements, or because of increased sensitivity of the wavefunctions to an electric field due to decreased ionicity [49].

The calculated BEC in Cartesian coordinates for the atoms of both compounds in the aragonite, calcite, and γ -phase structures are given in tables 10–12, respectively. Here, the z -axis is along the normal direction of the carbonate or nitrate groups where a ferroelectric switching is anticipated. We observe that BEC of cations (Ca or K) for all compounds in all

Table 12. Calculated BEC of the atoms in CaCO₃ and KNO₃ in the γ -phase structure.

Atom	CaCO ₃	KNO ₃
Ca/K	$\begin{pmatrix} 2.453 & & \\ & 2.453 & \\ & & 2.197 \end{pmatrix}$	$\begin{pmatrix} 1.094 & & \\ & 1.094 & \\ & & 1.043 \end{pmatrix}$
C/N	$\begin{pmatrix} 3.021 & & \\ & 3.021 & \\ & & 0.332 \end{pmatrix}$	$\begin{pmatrix} 2.814 & & \\ & 2.814 & \\ & & 0.180 \end{pmatrix}$
O	$\begin{pmatrix} -1.5436 & -0.4865 & -0.0273 \\ -0.4865 & -2.1054 & -0.0473 \\ -0.0313 & -0.0542 & -0.8428 \end{pmatrix}$	$\begin{pmatrix} -1.0040 & -0.5175 & -0.0101 \\ -0.5175 & -1.6016 & -0.0175 \\ -0.00003 & -0.00005 & -0.4077 \end{pmatrix}$
	$\begin{pmatrix} -2.3863 & & 0.0546 \\ & -1.2627 & \\ 0.0625 & & -0.8428 \end{pmatrix}$	$\begin{pmatrix} -1.9004 & & 0.0203 \\ & -0.7052 & \\ 0.00006 & & -0.4077 \end{pmatrix}$
	$\begin{pmatrix} -1.5436 & 0.4865 & -0.0273 \\ 0.4865 & -2.1054 & 0.0473 \\ -0.0313 & 0.0542 & -0.8428 \end{pmatrix}$	$\begin{pmatrix} -1.0040 & 0.5175 & -0.0101 \\ 0.5175 & -1.6016 & 0.0175 \\ -0.00003 & 0.00005 & -0.4077 \end{pmatrix}$

Table 13. Eigenvalues of the Born effective tensor for the oxygen atoms in the carbonate or nitrate group.

Phase	CaCO ₃ (E_1, E_2, E_3)	KNO ₃ (E_1, E_2, E_3)
Aragonite	-2.263, -1.170, -0.921	-1.634, -0.567, -0.446
Calcite	-2.498, -1.218, -0.793	-1.891, -0.705, -0.394
γ -phase	-2.389, -1.263, -0.841	-1.900, -0.705, -0.408

structures are nearly isotropic and although for Ca it is somewhat larger, especially along the directions normal to the switching axis, the diagonal elements have a value close to the nominal charge of the corresponding atom. Secondly, only for the γ -phase structure, the non-diagonal elements are all zero for the cations. For the calcite structure, however, there is considerable non-diagonal effective charge, which may be an indication of some hybridization between the cation and the oxygen orbitals. The effective charges of the group atoms depend strongly on the hybridization of orbitals within the group and are found to be very anisotropic, as may be expected. Contrary to the anomalously large effective charges reported in transition metals containing ferroelectric oxides [48, 52, 53, 55], in all structures and compounds studied, including ferroelectric KNO₃, we find the BEC of group atoms to be smaller than their nominal charge. The giant BECs in the above-mentioned oxides are found to occur along the metal–oxygen bonds and are very sensitive to bond distance, which can be attributed to strong covalent interactions between transition metal and oxygen atoms.

The BEC of central atoms in the group is smaller from the nominal charge (C^{4+} , N^{5+}) at least by 23% for C and 44% for N. In addition, there is almost an order of magnitude difference in the effective charges of C/N atoms within the plane and normal to the plane of the group, the latter being smaller. The same observation applies to O atoms as well, such that BEC along the switching direction is very small compared to BEC along directions within the plane of the group. All observations of these calculations, agree with the experimental findings reported in the literature for calcite–CaCO₃ and aragonite–KNO₃ [56].

Inspection of the eigenvalues given in table 13 and the eigenvectors of the effective charge tensor for the O atoms within the groups clearly reveals the anisotropy. It can be seen that the compound basis eigenvalues are quite similar to each other irrespective of the structure,

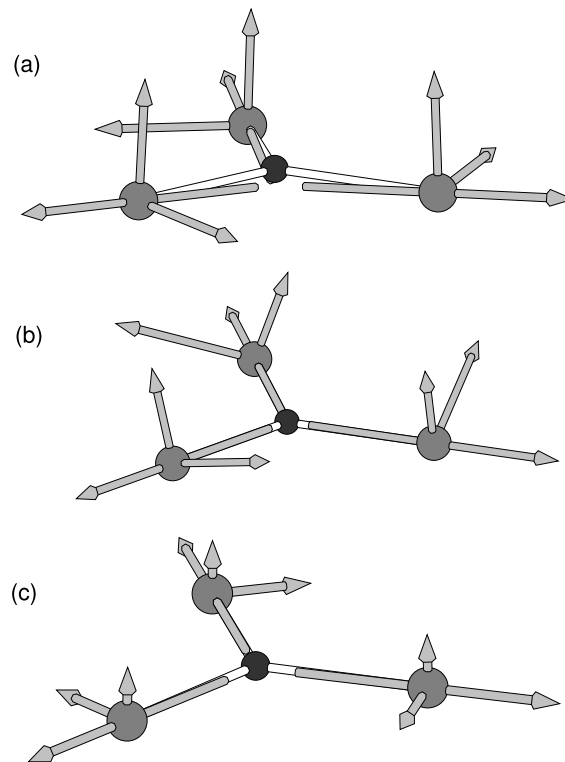


Figure 13. Eigenvector plots for the oxygen atoms within the group for (a) aragonite- CaCO_3 , (b) calcite- CaCO_3 and (c) γ -phase KNO_3 . The black circle represents the centre atom, carbon or nitrogen, and the grey circles represent the oxygen atoms in the carbonate or nitrate group.

except the third eigenvalue in the aragonite structure, which corresponds to the eigenvector that is approximately normal to the group plane. It is such that the third eigenvalue in the aragonite structure for both compounds is larger than the corresponding value in other structures relative to the largest eigenvalue in that structure. Moreover, all three eigenvalues are considerably larger in all structures of CaCO_3 than in KNO_3 . The associated eigenvectors clarify this picture further. In figure 13, the plots of the eigenvectors for the O atoms within the group were given for aragonite- CaCO_3 , calcite- CaCO_3 and γ -phase KNO_3 . It can be clearly seen that in all cases the largest eigenvector is along the bond between O and either C or N atom that is at the centre of the group and the second largest vector is perpendicular to the first one, the two being coplanar with the plane of the group in the γ -phase structure only. In other structures, the plane formed by the two largest eigenvectors is non-coplanar, indicating that an out-of-plane covalent hybridization between the group atoms (mostly O) and the cations has occurred.

Finally, we compute the energy variation of all the structures in both compounds with respect to polarization from which various properties can be derived. The ferroelectric instability, if it exists, can be identified from $E(\mathbf{P})$, where E is the energy variation with respect to polarization \mathbf{P} , with the occurrence of a more stable configuration at non-zero polarizations. As was stated earlier [9], for the γ -phase of KNO_3 , the change of polarization from negative to positive was found to be due to the movement of the NO_3 group of atoms parallel to the c -axis, accompanied by a 60° rotation of this group in their plane. There is a similar mechanism

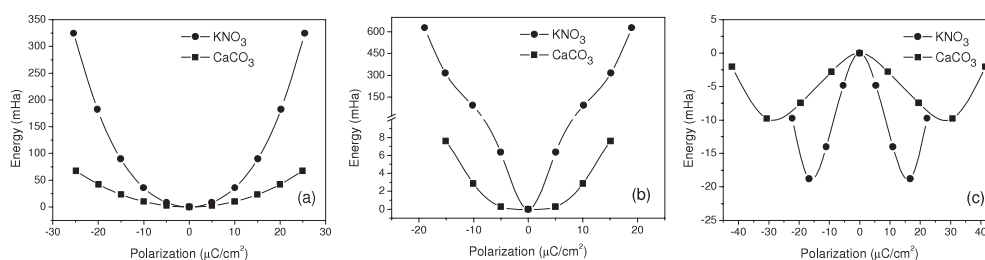


Figure 14. Energy versus polarization curves for CaCO_3 and KNO_3 in (a) aragonite, (b) calcite and (c) γ -phase structures.

for polarization in the case of calcite structure, where the movement of the carbonate group along the c -axis is accompanied by the rotation of it. This time, however, the groups lying below and above the cation layer along the c -axis rotate clockwise and counter-clockwise, respectively, about their normal axis, while they move up and down with an increase in the bond length between O and the C/N atoms. Lastly, in the aragonite structure there is the up and down movement of the group layer as a whole without any individual rotation of the groups. In figure 14, the crystal energy versus polarization maps are given for aragonite, calcite and γ -phase compounds, where in the calculations the lattice volume was set constant.

As can be seen from figure 13(c), only for the γ -phase structure is a double-well potential behaviour predicted; the main characteristic of ferroelectricity. In other structures of CaCO_3 and KNO_3 (aragonite and calcite) rotation and/or the motion of the groups do not yield any stable configuration at non-zero polarizations. The spontaneous polarization, the difference in polarizations between the configurations under zero electric field (non-polar state) and at the polarized state giving the lowest energy, was calculated for the γ -phase KNO_3 as $16.6 \mu\text{C cm}^{-2}$, which is very close to the value calculated by Dieguez and Vanderbilt [9]. Similarly, the calculated spontaneous polarization for γ -phase CaCO_3 is $30.6 \mu\text{C cm}^{-2}$; almost twice as much as the spontaneous polarization in γ -phase KNO_3 . Furthermore, the differences in energies between the polarized and non-polar state, i.e. the depth of the well in the $E(\mathbf{P})$ curves are found to be 18.8 mHa and 9.8 mHa for KNO_3 and CaCO_3 , respectively.

The γ -phase should be ferroelectric as it appears possible to switch it from one polarization state to the other by applying an electric field that will overcome the energy barrier between the states with opposite polarization. Therefore, the energy barrier or the well-depth in the potential, in a manner, characterizes the coercive field in the hysteretic behaviour of the ferroelectric. Our results show that polarization switching in CaCO_3 should occur at a much lower applied electric field compared to KNO_3 . We note that while the γ -phase of CaCO_3 is unstable and the calculated spontaneous polarizations may vary considerably since the theoretically found unit cell volumes (at least for the existing γ -phase KNO_3) may be smaller than the experimental values, its existence would be consistent with the existence of metastable KNO_3 .

6. Conclusions

In this study, we comparatively investigated the structural stability, electronic structure, bonding, and ferroelectric properties of CaCO_3 and KNO_3 compounds using first-principles DFT calculations. The calcite phase of CaCO_3 was found to be the ground state in this compound in agreement with experimental observations, whereas an aragonite structure, similar to that of KNO_3 was found to be slightly unstable, because of the large relaxation of the loosely packed crystal structures in DFT calculations. An electronic structure and orbital

hybridization analyses of the constituent atoms reveal that the N–O bond in the nitrate group is more covalent than the C–O bond in the carbonate, probably making the N–O bond length be slightly shorter than the C–O bond. Furthermore, the nitrate or the carbonate groups in the γ -phase were found to be almost in purely ionic interaction with the cations forming a layer of triangular networks above and below the groups. In calcite and aragonite structures, however, the Mulliken population analysis, charge density distribution plots, and the Born effective charge tensors reveal that there is some covalency between the O atoms of the groups and the cations. In the calcite structure, this causes the groups to align themselves between the layers of cations in such a way that each O in the group is attached to a cation from above and below with equal distance bonds in opposite directions that balance each other. This directional picture of bonding of the group to the surroundings makes the group locate itself just at the half distance between these layers. Any applied electric field that causes the rotation and/or the vertical motion of the group breaks the high symmetry configuration with an increased energy of the crystal, thus resulting in non-switching (non-ferroelectric) behaviour.

The spontaneous polarization in γ -phase KNO_3 and CaCO_3 were calculated to be 16.6 and 30.6 $\mu\text{C cm}^{-2}$, respectively, where in the latter system, switching seems to be achieved easily with a lower coercive field; however for neither of these compounds is this crystal structure stable. γ -phase KNO_3 is metastable and ferroelectricity can be induced in thin films via internal stresses, but to date ferroelectricity in CaCO_3 has never been observed. Consistent with KNO_3 , the calcite and aragonite forms of CaCO_3 will not exhibit ferroelectric behaviour. It is conjectured that γ -phase CaCO_3 can be made through the addition of dopants and internal stresses (as has been done with KNO_3) such that the carbonate groups become more compact and/or the cage formed by the Ca ions becomes larger. In this way, the covalent interaction can be avoided between the carbonate groups and the cations which makes the group locate itself exactly halfway between the cation layers. This covalent interaction may actually be the reason why the calcite structure is preferred over the γ -phase structure in CaCO_3 .

There may be several ways to lessen this covalent interaction; one way may be the substitution of Ca with larger ions to increase the size of the cage, towards stabilizing the aragonite structure over the calcite structure as carbonates of Ba and Sr that are larger than Ca and are of aragonite type [57]. This may assist in the transition to the γ -phase, since the ground state of KNO_3 is aragonite; a precursor to the ferroelectric γ -phase. In KNO_3 , if K is replaced with a smaller ion such as Na, then from the above understanding one may expect the nitrate to go towards a calcitic structure, which is actually the case for pure LiNO_3 and NaNO_3 . Substitution of C may help as well, resulting in stronger covalent bonds between O so that the bond length decreases. Finally, another way to achieve a carbonate γ -phase would be to constrain the calcite lattice, preferably by putting the basal plane of the hexagonal calcite in tension in epitaxial growth of thin films of CaCO_3 . Experiments are currently underway to substantiate these conjectures.

Acknowledgments

All DFT calculations reported in this study were carried out at the Turkish Academic Network and Information Centre (ULAKBIM) High Performance Computing Center of the Turkish Scientific and Technical Research Council (TÜBİTAK), which is greatly appreciated. The work at UConn was supported by the US Army Research Office through grant W911NF-05-1-0528.

References

- [1] Nolta J P and Schubring N W 1962 *Phys. Rev. Lett.* **9** 285
- [2] Sawada S, Nomura S and Fujii S 1958 *J. Phys. Soc. Japan* **13** 1549

- [3] Adams D M, Hatton P D, Heath A E and Russell D R 1988 *J. Phys. C: Solid State Phys.* **21** 505–15
- [4] Aresti A, Meloni F, Pegna G G and Serra M 1983 *Phys. Status Solidi a* **80** 119–26
- [5] Christensen A N, Norby P, Hanson J C and Shimada S 1996 *J. Appl. Crystallogr.* **29** 265–9
- [6] Harris M J 1992 *Solid State Commun.* **84** 557–61
- [7] Leong J T and Emrick R M 1971 *J. Phys. Chem. Solids* **32** 2593
- [8] Scott J F, Zhang M S, Godfrey R B, Araujo J and McMillan L 1987 *Phys. Rev. B* **35** 4044
- [9] Dieguez O and Vanderbilt D 2006 *Phys. Rev. Lett.* **96** 56401
- [10] Lu H M and Hardy J R 1990 *Ferroelectrics* **111** 43–7
- [11] Lu H M and Hardy J R 1991 *Phys. Rev. B* **44** 7215
- [12] Bridgman P W 1916 *Proc. Am. Acad. Sci.* **51** 581
- [13] Pistorius C W F T 1976 *Prog. Solid State Chem.* **11** 1
- [14] Rapaport E and Kennedy G C 1965 *J. Phys. Chem. Solids* **26** 1995
- [15] Tahvonen P E 1947 *Ann. Acad. Sci. Fenn. Ser. A* **44** 1
- [16] Nimmo J K and Lucas B W 1976 *Acta Crystallogr. B* **32** 1968
- [17] Barth T F W 1939 *Z. Phys. Chem. B* **43** 448
- [18] Sawada S, Nomura S and Asao Y 1961 *J. Phys. Soc. Japan* **16** 2486
- [19] Sai N, Rabe K M and Vanderbilt D 2002 *Phys. Rev. B* **66** 104108
- [20] Yanagi T 1965 *J. Phys. Soc. Japan* **20** 1351
- [21] Chen A and Chernow F 1967 *Phys. Rev.* **154** 493
- [22] Dickens B and Bowen J S 1971 *J. Res. Nat. Bur. Stand. A* **75** 27
- [23] Nimmo J K and Lucas B W 1973 *J. Phys. C: Solid State Phys.* **6** 201
- [24] Maslen E N, Streltsov V A, Streltsova N R and Ishizawa N 1995 *Acta Crystallogr. B* **51** 929
- [25] Liu J, Duan C G, Ossowski M M, Mei W N, Smith R W and Hardy J R 2001 *Phys. Chem. Minerals* **28** 586
- [26] Oganov A R, Glass C W and Ono S 2006 *Earth Planet. Sci. Lett.* **241** 95
- [27] Baroni S, de Gironcoli S, dal Corso A and Giannozzi P 2001 *Rev. Mod. Phys.* **73** 515
- [28] King-Smith R D and Vanderbilt D 1993 *Phys. Rev. B* **47** 1651
- [29] Resta R 1992 *Ferroelectrics* **136** 51
- [30] ABINIT <http://www.abinit.org>
- [31] Dawber M, Rabe K M and Scott J F 2005 *Rev. Mod. Phys.* **77** 1083
- [32] Resta R 2003 *Modelling Simul. Mater. Sci. Eng.* **11** R69
- [33] Ordejon P, Artacho E and Soler J M 1996 *Phys. Rev. B* **53** R10441
- [34] Soler J M, Artacho E, Gale J D, Garcia A, Junquera J, Ordejon P and Sanchez-Portal D 2002 *J. Phys.: Condens. Matter* **14** 2745
- [35] Troullier N and Martins J L 1991 *Phys. Rev. B* **43** 1993
- [36] Souza I, Iniguez J and Vanderbilt D 2002 *Phys. Rev. Lett.* **89** 117602
- [37] Veithen M, Gonze X and Ghosez P 2005 *Phys. Rev. B* **71** 125107
- [38] Fuchs M and Scheffler M 1999 *Comput. Phys. Commun.* **119** 67
- [39] Dove M T and Powell B M 1989 *Phys. Chem. Minerals* **16** 503
- [40] Stokes H T, Hatch D M and Campbell B J 2007 *Isotropy* <http://stokes.byu.edu/isotropy.html>
- [41] Catti M, Pavese A, Dovesi R and Saunders V R 1993 *Phys. Rev. B* **47** 9189
- [42] Catti M, Pavese A, Apra E and Roetti C 1993 *Phys. Chem. Minerals* **20** 104
- [43] Skinner A J, LaFemina J P and Jansen H J F 1994 *Am. Mineral.* **79** 205
- [44] Wheeler R A, Whangbo M H, Hughbanks T, Hoffmann R, Burdett J K and Albright T A 1986 *J. Am. Chem. Soc.* **108** 2222
- [45] Cohen R E and Krakauer H 1990 *Phys. Rev. B* **42** 6416
- [46] Inbar I and Cohen R E 1996 *Phys. Rev. B* **53** 1193
- [47] Ghosez P, Michenaud J-P and Gonze X 1998 *Phys. Rev. B* **58** 6224
- [48] Zhong W, King-Smith R D and Vanderbilt D 1994 *Phys. Rev. Lett.* **72** 3618
- [49] Waghmare U V, Spaldin N A, Kandpal H C and Seshadri R 2003 *Phys. Rev. B* **67** 125111
- [50] Ghosez P, Gonze X and Michenaud J-P 1996 *Europhys. Lett.* **33** 713
- [51] Weber M J 2003 *Handbook of Optical Materials* (Boca Raton, FL: CRC Press)
- [52] Wang C Z, Yu R and Krakauer H 1996 *Phys. Rev. B* **54** 11161
- [53] Resta R, Posternak M and Baldereschi A 1993 *Phys. Rev. Lett.* **70** 1010
- [54] Posternak M, Resta R and Baldereschi A 1994 *Phys. Rev. B* **50** 8911
- [55] Ghosez P, Gonze X, Lambin P and Michenaud J-P 1995 *Phys. Rev. B* **51** 6765
- [56] Brehat F, Wyncke B and Gervais F 1989 *J. Phys.: Condens. Matter* **1** 9001
- [57] Chang L L Y, Howie R A and Zussman J 1998 *Rock Forming Minerals vol 5B Non-Silicates: Sulphates, Carbonates, Phosphates, Halides* (London: Geological Society)